Int. J. Heat Mass Transfer. Vol. 16, pp. 1425–1438. Pergamon Press 1973. Printed in Great Britain

DEVELOPMENT OF FREE CONVECTION AXIAL FLOW THROUGH A TUBE BUNDLE

LEONARD P. DAVIS*

and

JOSEPH J. PERONA

Department of Chemical and Metallurgical Engineering, University of Tennessee, Knoxville, Tennessee 37916, U.S.A.

(*Received* 18 *February* 1972 *and in revised form* 26 *October* 1972)

Abstract—An open tube bundle is immersed in a fluid. The tubes, which are oriented vertically, generate heat and the fluid enters the bottom of the bundle with uniform velocity and temperature and flows up through the bundle outside of the tubes. The flow is assumed to be stable and laminar. The thermal boundary layer equations were solved for pitch-to-diameter ratios of 1·2–2·0 with air as the fluid, allowing density, viscosity and thermal conductivity to vary with temperature.

Local Nusselt numbers were correlated with a modified Graetz number and showed parametric dependence on both pitch-to-diameter ratio and dimensionless flow rate.

Correlations of dimensionless flow rate with dimensionless tube bundle length were unaffected by considerations of variable physical properties provided the dimensionless flow rates were evaluated at outlet conditions.

Experiments performed on two tube bundles (pitch-to-diameter ratios of 1·68 and 2·03) under the condition of constant wall heat flux verified the theoretical predictions of Nusselt numbers. Predicted flow rates were displaced below the predicted curves due to constrictions in the flow area caused by the tube spacers.

NOMENCLATURE

A, heat transfer area;

a, grouping of terms defined by equation (34);

b, tube radius;

C_p, heat capacity;

D, tube diameter;

F, dimensionless volumetric flow rate;

F_0, inlet value of F;

F', outlet value of F;

f, volumetric flow rate;

f_0, inlet value of f;

Gr, Grashof number;

Gr^*, modified Grashof number

$$= \frac{g\beta_0 \Delta t b^4}{l\nu_0^2};$$

g, acceleration due to gravity;

h_{local}, heat transfer coefficient based on local temperature difference;

k, thermal conductivity of fluid at local temperature;

k_0, k evaluated at ambient temperature;

L, dimensionless length $= 1/Gr^*$;

L^*, modified dimensionless length

$$= \frac{L}{(R_m^2 - 1)^4};$$

l, length of tube bundle;

m, exponent describing temperature dependence of k;

Nu, Nusselt number;

n, exponent describing temperature dependence of μ;

P, dimensionless pressure defect

$$= \frac{p'b^4}{\rho_0 l^2 \nu_0^2 Gr^{*2}};$$

PDR, pitch-to- diameter ratio;

* Now with Tennessee Eastman Company, Kingsport, Tennessee.

Pr, Prandtl number;
p, pressure;
p_0, hydrostatic pressure of fluid at ambient temperature;
p', pressure defect $= p - p_0$;
Q, dimensionless rate of heat removal up to a particular level in the bundle;
Q', Q evaluated at exit;
q, rate of heat removal up to a particular level in the bundle;
R, dimensionless radial position $= r/b$;
Re, Reynolds number;
R_m, dimensionless value of r_m;
r, radial position;
r_m, radius of area affected by tube;
T, dimensionless temperature $= \dfrac{t - t_0}{\Delta t}$;
T_m, dimensionless mixing-cup temperature;
T_m', T_m evaluated at exit;
T_w, dimensionless wall temperature;
$\overline{T}$, absolute temperature;
$\overline{T}_0$, ambient value of $\overline{T}$;
t, temperature;
t_m, mixing-cup temperature;
t_0, ambient temperature;
t_w, wall temperature;
Δt, characteristic temperature difference;
U, dimensionless velocity in axial direction $= \dfrac{b^2 u}{l\nu_0 Gr^*}$;
U_m, mean value of U;
U_0, inlet value of U;
u, velocity in z-direction;
u_0, inlet value of u;
V, dimensionless radial velocity component $= bv/\nu_0$;
v, radial velocity component;
Z, dimensionless axial position $= z/lGr^*$
z, axial position.

Greek letters

β, thermal coefficient of volume expansion;
β_0, value of β at ambient conditions;
μ, absolute viscosity;
μ_0, ambient value of μ;
ν, kinematic viscosity;
ν_0, ambient value of ν;
ξ, $\beta_0 \Delta t$;
ρ, fluid density;
ρ_0, ambient value of ρ.

INTRODUCTION

THE EFFECTS of free convection in vertical tube bundles are significant in engineering problems involving spent nuclear fuel assemblies. An analysis of flow development of air in a vertical tube was carried out previously and the results compared with the experimental work of Elenbaas [1]. The present analysis in many respects is similar to that for the tube, but differs not only in the geometry of the channel but also in that the variations of many fluid properties with temperature were taken into account.

Specifically, the study entails solving the thermal boundary-layer equations in cylindrical coordinates via a finite difference technique. All fluid properties, except heat capacity and Prandtl number, were allowed to vary with temperature. Calculations were made for the velocity and temperature profiles; and from these, various quantities such as rate of heat removal, Nusselt numbers, and correlations of volumetric flow rate as a function of a modified Grashof number were obtained. In addition, an analytical solution was obtained for fully developed flow.

With a situation as mathematically difficult as in-line flow through a tube bundle, some simplifying assumptions must be made. Edge effects are ignored by assuming an infinite array of tubes in the bundle. It is then possible to focus attention to a single tube and analyze the flow and heat transfer processes taking place due to the influence of this one tube.

Following a procedure used by Friedland and Bonilla [2] for a tube bundle with an equilateral triangular pitch, a hexagon can be circumscribed about a tube to represent the flow area and fluid assignable to that particular tube.

It is assumed that this situation can be approximated closely enough by replacing the hexagon with a circle of equal area (thus maintaining the same hydraulic radius as before) with velocity and temperature profiles that would be obtained in the case of the shear stress and heat flux dropping to zero at the circumference of the circle.

THE CONSERVATION EQUATIONS

In general, the flow of fluids can be described by the continuity, momentum, and energy equations. In addition to the usual boundary layer assumptions previously made for the tube [1], the following assumptions are made:

(a) ρ is a function of temperature only as described by the ideal gas law.

(b) μ is a function of temperature only and its variation is described by $\mu = \mu_0(\bar{T}/\bar{T}_0)^n$.

(c) k is a function of temperature described by a similar variation: $k = k_0(\bar{T}/\bar{T}_0)^m$.

(d) The heat capacity and Prandtl number are constant.

With these assumptions and substituting the dimensionless variables defined in the Nomenclature, the equations become:

Continuity

$$\frac{\partial U}{\partial Z} + \frac{\partial V}{\partial R} + \frac{V}{R} = \beta(\Delta t)\left[V\frac{\partial T}{\partial R} + U\frac{\partial T}{\partial Z}\right], \quad (1)$$

which can be rewritten as

$$\frac{\partial U}{\partial Z} + \frac{\partial V}{\partial R} + \frac{V}{R} = \frac{\xi}{\xi T + 1}\left[V\frac{\partial T}{\partial R} + U\frac{\partial T}{\partial Z}\right], \quad (2)$$

where

$$\xi = \beta_0(\Delta t).$$

This substitution is possible since β, for an ideal gas, is the reciprocal of absolute temperature.

Momentum

Using the temperature variations for μ and k introduced earlier and noting that

$$\frac{\partial \mu}{\partial r} = \frac{\partial \mu}{\partial t}\frac{\partial t}{\partial r},$$

the momentum equation can be written as

$$U\frac{\partial U}{\partial Z} + V\frac{\partial U}{\partial R} = -(\xi T + 1)\frac{\partial P}{\partial Z} + T + (\xi T + 1)^{n+1}\left[\frac{\partial^2 U}{\partial R^2} + \frac{1}{R}\frac{\partial U}{\partial R}\right] + n(\xi T + 1)^n \xi \frac{\partial T}{\partial R}\frac{\partial U}{\partial R}. \quad (3)$$

Energy

Noting that as for μ, $\partial k/\partial r$ can be written as $(\partial k/\partial t)(\partial t/\partial r)$ the energy equation becomes

$$U\frac{\partial T}{\partial Z} + V\frac{\partial T}{\partial R} = \frac{1}{Pr}(\xi T + 1)^{m+1}\left[\frac{\partial^2 T}{\partial R^2} + \frac{1}{R}\frac{\partial T}{\partial R}\right] + \frac{m(\xi T + 1)^m \xi}{Pr}\left(\frac{\partial T}{\partial R}\right)^2. \quad (4)$$

Denoting the mass flow rate by $\bar{m}$ we see that if the initial velocity is termed u_0 then

$$\bar{m} = u_0\rho_0\pi(r_m^2 - b^2) = 2\pi\int_b^{r_m} u\rho r\,dr. \quad (5)$$

The initial volumetric flow rate is simply $\bar{m}/\rho_0$. At any position the flow rate is given by

$$f = 2\pi\int_b^{r_m} ur\,dr, \quad (6)$$

while the initial rate can be found at any level from

$$f_0 = 2\pi\int_b^{r_m} u\frac{\rho}{\rho_0} r\,dr. \quad (7)$$

The quantities f and f_0 can be put in terms of dimensionless variables to yield

$$F = \frac{f}{v_0 lGr^*\pi} = 2\int_1^{R_m} UR\,dR \quad (8)$$

and

$$F_0 = \frac{f_0}{v_0 lGr^*\pi} = 2\int_1^{R_m} \frac{UR}{(\xi T + 1)}\,dR. \quad (9)$$

F_0 is independent of changes in height and can provide a numerical check on the consistency of the results to be obtained from the finite difference solution. This quantity can also be related to the initial velocity as follows:

$$F_0 = \frac{u_0\pi(r_m^2 - b^2)}{v_0 lGr^*\pi} = U_0(R_m^2 - 1). \quad (10)$$

The boundary conditions for the solution of equations (2)–(4) can be expressed as follows for constant wall heat flux:

for $Z = 0$ and $1 < R \leqslant R_m$:

$$U = \frac{F_0}{(R_m^2 - 1)}, V = 0, T = 0; \quad (11)$$

for $R = 1$ and $Z > 0$:

$$U = 0, V = 0, \frac{\partial T}{\partial R} = \frac{-1}{(\xi T + 1)^m} \quad (12)$$

for $R = R_m$ and $Z \geqslant 0$:

$$\frac{\partial U}{\partial R} = 0, V = 0, \frac{\partial T}{\partial R} = 0; \quad (13)$$

for $Z = 0$ and $Z = L$: $P = 0$. (14)

Equation (12) follows quite naturally from Fourier's law written for $R = 1$:

$$\left(\frac{q}{A}\right)_w = -k\left(\frac{\partial t}{\partial r}\right)_w, \quad (15)$$

and from the definition of the characteristic Δt used in this work,

$$\Delta t = \frac{(q/A)_w b}{k_0}. \quad (16)$$

The local heat transfer coefficient is defined by

$$\left(\frac{q}{A}\right)_w = h_{\text{local}}(t_w - t_m), \quad (17)$$

and

$$\frac{h_{\text{local}} D}{k_0} = \frac{(q/A)_w D}{(t_w - t_m)k_0}. \quad (18)$$

Substituting the dimensionless variables into the last equation, it is found that

$$Nu_{\text{local}} = \frac{2}{T_w - T_m}. \quad (19)$$

The dimensionless heat absorbed per unit time can be shown to be

$$Q = \frac{qk_0}{\pi\rho_0 C_p l v_0 Gr^*(q/A)_w} = \frac{2Z}{Pr} \quad (20)$$

where

$$q = \int_b^{r_m} 2\pi C_p \rho u(t - t_0) r \, dr. \quad (21)$$

Note that the above expression for Nu is in terms of k_0. To obtain the local Nusselt number in terms of k evaluated at the local mean temperature, equation (19) is divided by $(1 + \xi T_m)^m$.

For constant heat flux at the tube walls, the conventional concept of developed flow must be modified. Since the driving force is sustained (i.e. the difference in temperature of the wall and the fluid does not approach zero), it is possible to specify hydrodynamically and thermally developed flow by defining $V = 0$ and $\partial U/\partial Z = 0$. These conditions, however, are adequate only for flow with non-variable density. When density varies, as in this case, $\partial U/\partial Z$ can never equal zero. Therefore, one must be content with the condition when $V = 0$ as describing a pseudo-hydrodynamically developed flow. Thermally developed flow is achieved when $\partial T/\partial Z$ equals a constant. With the simplification usually wrought when one considers developed flow an analytical solution can be obtained. However, this situation is not true in the present investigation because of the additional non-linearities introduced by considering ρ, μ and k to be variable with temperature.

The continuity, momentum and energy equations for this pseudo-developed flow situation are, respectively:

$$\frac{\partial U}{\partial Z} = \frac{\xi}{\xi T + 1} U \frac{\partial T}{\partial Z}, \quad (22)$$

$$U\frac{\partial U}{\partial Z} = -(\xi T + 1)\frac{\partial P}{\partial Z} + (\xi T + 1)^{n+1} \times \left[\frac{\partial^2 U}{\partial R^2} + \frac{1}{R}\frac{\partial U}{\partial R}\right] + T$$

$$+ n\xi(\xi T + 1)^n \frac{\partial T}{\partial R}\frac{\partial U}{\partial R}, \quad (23)$$

$$U\frac{\partial T}{\partial Z} = \frac{1}{Pr}(\xi T + 1)^{m+1}\left[\frac{\partial^2 T}{\partial R^2} + \frac{1}{R}\frac{\partial T}{\partial R}\right] + \frac{m\xi(\xi T + 1)^m}{Pr}\left(\frac{\partial T}{\partial R}\right)^2. \quad (24)$$

As the above equations stand, they are hopelessly non-linear. The problem is to remove the non-linearity and still retain some semblance of temperature dependent fluid properties. This criterion can be achieved by considering these properties to be dependent upon the mixing-cup temperature only, and neglecting their variation with temperature across the flow channel. That is,

$$\frac{\partial \mu}{\partial r} = \frac{\partial k}{\partial r} = 0 \text{ and } (\xi T + 1) = (\xi T_m + 1). \quad (25)$$

With these assumptions, equations (22)–(24) become

$$\frac{\partial U}{\partial Z} = \frac{\xi}{\xi T_m + 1} U\frac{\partial T}{\partial Z}, \quad (26)$$

$$U\frac{\partial U}{\partial Z} = -(\xi T_m + 1)\frac{\partial P}{\partial Z} + T + (\xi T + 1)^{n+1} \times \left[\frac{\partial^2 U}{\partial R^2} + \frac{1}{R}\frac{\partial U}{\partial R}\right], \quad (27)$$

and

$$U\frac{\partial T}{\partial Z} = \frac{(\xi T_m + 1)^{m+1}}{Pr}\left[\frac{\partial^2 T}{\partial R^2} + \frac{1}{R}\frac{\partial T}{\partial R}\right]. \quad (28)$$

The term $U\,\partial U/\partial Z$ on the left hand side of equation (27) also poses a problem of non-linearity. Noting that this term drops out for non-variable density, and since variations of physical properties are assumed to be a function of mixing-cup temperature only, it seems proper to replace $U\,\partial U/\partial Z$ by $U_m\,\partial U_m/\partial Z$. Likewise, in the continuity equation U_m will be used in place of U. The variation of T with R will not change with changing level in the channel; that is, $T(R_1, Z_1) = \text{constant } xT(R_1, Z_2)$. Hence, $\partial T/\partial Z$ can be replaced by $\partial T_m/\partial Z$.

The continuity equation can now be written as

$$\frac{\partial U_m}{\partial Z} = \frac{\xi}{\xi T_m + 1} U_m \frac{\partial T_m}{\partial Z}, \quad (29)$$

which when solved for U_m yields

$$U_m = U_0(\xi T_m + 1); \quad (30)$$

however,

$$U_0 = \frac{F_0}{(R_m^2 - 1)}$$

and $F = F_0(\xi T_m + 1)$.
Therefore,

$$U_m = \frac{F}{(R_m^2 - 1)}.$$

Solving the equation of motion for T gives

$$T = U_m\frac{\partial U_m}{\partial Z} + (\xi T_m + 1)\frac{\partial P}{\partial Z} - (\xi T_m + 1)^{n+1}(\nabla^2 U), \quad (31)$$

where

$$\nabla^2 = \frac{1}{R}\frac{\partial}{\partial R}\left(R\frac{\partial}{\partial R}\right). \quad (32)$$

Turning now to the energy equation, it is found by integrating from $R = 1$ to $R = R_m$ that

$$\frac{\partial T}{\partial Z} = \frac{2}{F_0 Pr}.$$

Making this substitution and substituting the expression for T in equation (31) into the energy equation yields

$$\nabla^4 U + a^4 U = 0, \quad (33)$$

where

$$a^4 = \frac{2}{F_0(1 + T_m)^{2+m+n}}. \quad (34)$$

The solution can be written as

$$U = G\,\text{ber}(aR) + H\,\text{bei}(aR) + M\,\text{ker}(aR) + N\,\text{kei}(aR). \quad (35)$$

The constants G, H, M and N can be evaluated by using the conditions:

$$U = 0 \text{ at } R = 1,$$

$$\frac{\partial U}{\partial R} = 0 \text{ at } R = R_m,$$

$$(1 + \xi T_m)F_0 = \int_1^{R_m} UR\,\mathrm{d}R,$$

and

$$\frac{\partial T}{\partial R} = 0 \text{ at } R = R_m.$$

Having the expression for velocity, the energy equation can now be solved for the temperature profile. Starting with equation (28) and substituting the expression for U from equation (35) gives the following:

$$\mathrm{d}\left(R\frac{\partial T}{\partial R}\right) = a^4[G\,\mathrm{ber}(aR) + H\,\mathrm{bei}(aR) + M\,\mathrm{ker}(aR) + N\,\mathrm{kei}(aR)] \times (\xi T_m + 1)^{n+1}R\mathrm{d}R. \quad (36)$$

If one integrates from $R = 1$ to $R = R$, it is found that

$$R\frac{\partial T}{\partial R} + \frac{1}{(1 + \xi T_m)^m} = a^3\{G[R\,\mathrm{bei}'(aR) - \mathrm{bei}'(a)] - H[R\,\mathrm{ber}'(aR) - \mathrm{ber}'(a)] + M[R\,\mathrm{kei}'(aR) - \mathrm{kei}'(a)] - N[R\,\mathrm{ker}'(aR) - \mathrm{ker}'(a)]\}(\xi T_m + 1)^{n+1}. \quad (37)$$

Upon rearranging and integrating again, the dimensionless temperature is

$$T = a^2\{G[\mathrm{bei}(aR) - \mathrm{bei}(a)] - H[\mathrm{ber}(aR) - \mathrm{ber}(a)] + M[\mathrm{kei}(aR) - \mathrm{kei}(a)] - N[\mathrm{ker}(aR) - \mathrm{ker}(a)]\}(\xi T_m + 1)^{n+1} - a^3[G\,\mathrm{bei}'(a) - H\,\mathrm{ber}'(a) + M\,\mathrm{kei}'(a) - N\,\mathrm{ker}'(a)](\xi T_m + 1)^{n+1}\,\ln R - \frac{\ln R}{(1 - \xi T_m)^m} + T_w. \quad (38)$$

The evaluation of T cannot be carried any further since there is no *a priori* knowledge of T_w. However, for purposes of comparing these results with those obtained from the numerical solution the above is sufficient, since T_w is available there.

NUMERICAL SOLUTIONS FOR DEVELOPING FLOW

A typical implicit-method finite difference solution was carried out. At a point along the channel the temperature distribution across the channel was calculated from the energy equation using axial and radial velocity components from the increment below. The axial velocity distribution was calculated from the momentum equation, and the radial velocity distribution from the continuity equation. The procedure is identical to that for the tube [1] and is given in detail in [3].

THEORETICAL RESULTS

The finite difference equations were solved for the velocity and temperature profiles at various stages of the flow development. From physical property data in *Chemical Engineers' Handbook* [4], the following values of the parameters for air were used:

$$Pr = 0{\cdot}7, n = 0{\cdot}768, m = 0{\cdot}857.$$

It was assumed that heat capacity and Prandtl number are constant. The logic behind these assumptions might be questioned because, if Pr is independent of temperature, then $C_p \propto (\overline{T}/\overline{T}_0)^{m-n}$. For moderately large changes in temperature (e.g. $\overline{T}/\overline{T}_0 = 2$) the resulting error in C_p is about 6 per cent. The results to be presented should be viewed with this discrepancy in mind.

The range of pitch-to-diameter ratios used in the calculations was 1·2–2·0. In each set of calculations, fifty increments were used in the radial direction while the increment size in the flow direction was changed for each level in the bundle. Changing ΔZ was done so as to have small increments near the entrance (less than

1/500 of the total dimensionless length) where changes take place most rapidly and yet permits completion of the calculations without an excessive amount of computer time, since larger increments are used further downstream.

The nature of the results is such that constant fluid properties need not be considered separately from variable fluid properties. For ξ equal to zero and a given pitch-to-diameter ratio, log F (or log F_0) vs log L yields a straight line with slope approximately equal to 0·515. Of course, the parametric behaviour for varying PDR is observed. Of considerably more importance is that a plot of F' (the prime denotes outlet value of F) vs. L for a given PDR and various values of ξ results in a single line independent of ξ. This is significant in that one need not search for a reference temperature which allows representation of various heating rates on a single curve as was done in the work of Sparrow and Gregg [5]. The relationship of F' as a function of L is shown in Fig. 1 for PDR ranging from 1·2 to 2·0. The dimensionless quantity representative of the total heat transfer, Q' is also shown as one curve for all PDR and all ξ, and as noted in equation (20) is equal to $2\,L/Pr$.

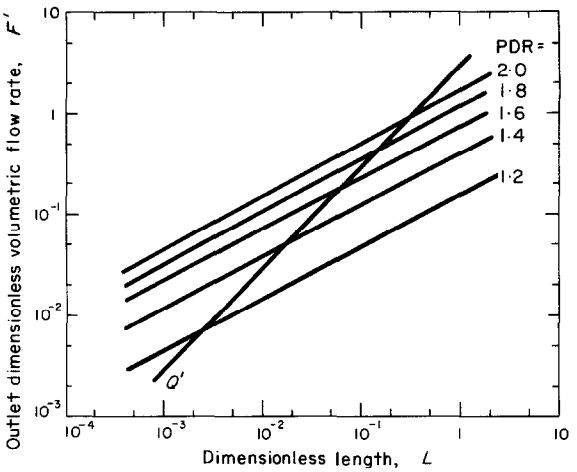

FIG. 1. Dimensionless outlet flow rate as a function of dimensionless length showing parametric dependence on PDR. Constant wall heat flux.

Local Nusselt numbers based on diameter and with k evaluated at the local mixing-cup temperature are plotted as a function of a modified Graetz number in Fig. 2. Not only are the curves parametric in PDR, but also exhibit dependence on F'. This dependence is most pronounced for Nu approaching its asymptotic

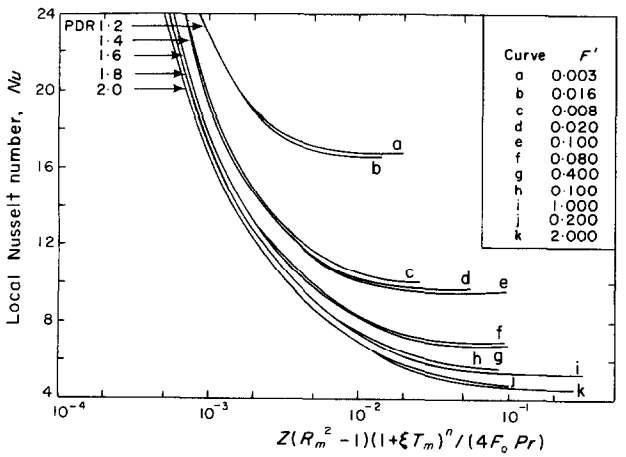

FIG. 2. Local Nusselt number as a function of modified Graetz number showing parametric dependence on PDR and F'. Constant wall heat flux.

value and is a result of the effect that heat transfer has on the velocity and temperature profiles. Small values of F' (large heating rates and/or large radii) produce relatively flat velocity and temperature profiles even far from the entrance while the velocity and temperature profiles for large values of F' approach the shape usually associated with forced convection heat transfer.

The general shape of the curves is readily explained by considering the definition of Nu in terms of the dimensionless variables,

$$Nu = \frac{2}{(T_w - T_m)}.$$

Right at the entrance, the tube surface temperature is nearly equal to the mean fluid temperature and finally assumes a linear variation paralleling the air temperature. Thus, Nu should be very large near the entrance and approach a constant value near the exit as in Fig. 2.

Evaluating both the ordinate and abscissa at the bulk temperature removes most of the parametric behaviour associated with variations in ξ. For example, consider the case of PDR = 1·4 and $F' = 0{\cdot}0246$. The changes in Nu brought about by varying ξ from 0·0 to 0·4 were less than one per cent at the point where calculations for $\xi = 0{\cdot}0$ were terminated. Some parametric behaviour remains in that larger values of the abscissa are required for the larger value of ξ.

APPARATUS

The data in this investigation were obtained from two triangular-pitch tube bundles. These tube bundles differ only in pitch-to-diameter ratios—one being 1·68: the other, 2·03. Other pertinent characteristics of the bundle are as follows:

Overall length	48·5 in.
Tube outside diameter	$\frac{5}{8}$ in.
Wall thickness	0·048 in.
Number of tubes in the bundle	42

The tubes of 304 stainless steel were arranged in seven staggered rows of six tubes per row so as to produce a bundle with an overall cross section that was almost square.

In order to investigate in-line or parallel flow through the tube bundle, it was essential that the ends be kept as open as possible. To accomplish this, special end pieces were constructed of short (one-half inch long) copper tubing and tubing couplings. The couplings used were standard $\frac{5}{8}$-in. i.d. rolled-stop copper coupling cut in half at the rolled stop. These, serving as holders for the stainless steel tubes, were held in the proper triangular pitch configuration by brazing them to the pieces of copper tubing.

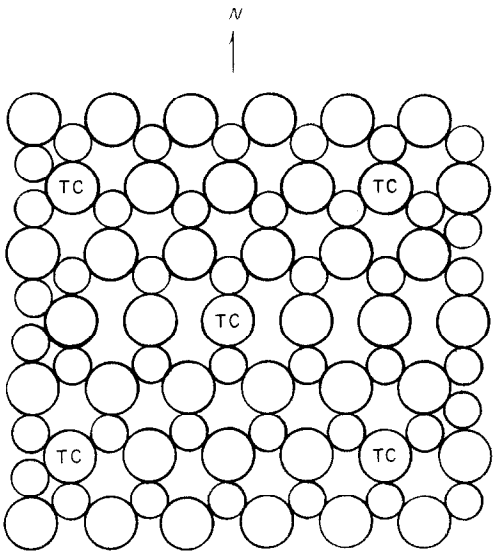

FIG. 3. Schematic diagram of end piece showing tube holders and spacers.

The resulting end piece is shown schematically in Fig. 3. The smaller pitch-to-diameter ratio was achieved by using spacers of $\frac{1}{2}$-in. dia copper tubing while the larger ratio was obtained by substituting $\frac{3}{4}$-in. tubing. By using these end pieces, only one set of tubes had to be fitted with heating elements since the tubes could be removed from the first bundle and placed in the second.

Each of the forty-two tubes in the bundle was fitted with an electrical heating element which

consisted of a four-hole ceramic thermocouple tube threaded with approximately 16 ft of nichrome wire (12·6 mil). The ceramic "spaghetti" was 4 ft long and $\frac{5}{16}$ in. dia. The ends of the nichrome wire were connected to small brass screws which were allowed to extend beyond the end of the stainless steel tube when the heating elements were cemented in place and served to connect the heating elements to the power source. Ceramic cement was used to hold the ends on the heating elements in place. To eliminate convection currents between the heating element and the stainless steel tube this annular space was filled with granular magnesium oxide. A schematic diagram of a representative tube is presented in Fig. 4.

The sides of the bundle were enclosed with $\frac{1}{2}$-in. Transite asbestos insulation. Fiber glass batting ($3\frac{7}{8}$-in. thick) was used next, followed by an outer shell of $\frac{3}{4}$-in. plywood. The entire assembly was mounted on a uni-strut frame so that the bottom was approximately 18 in. above a grate floor. Further details of the apparatus are given in [3].

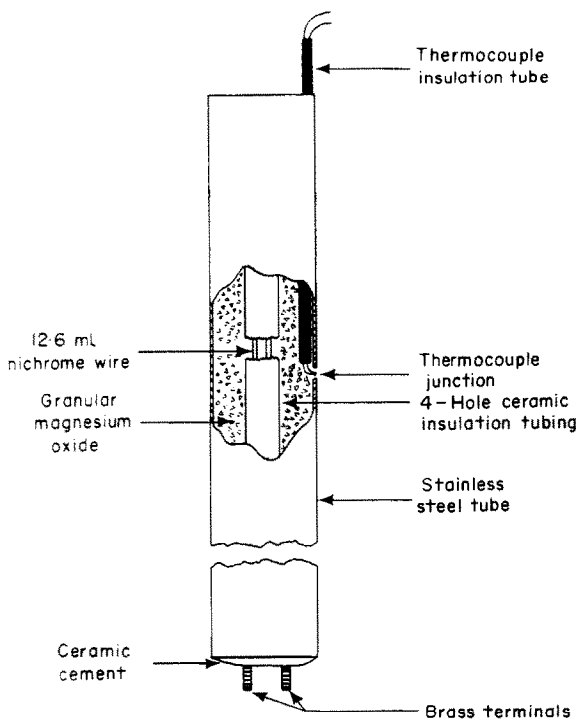

FIG. 4. Details of a representative tube.

In the experimental runs the following variables were measured:

1. Electrical power input,
2. Tube wall temperature at selected locations,
3. Outlet mixing-cup temperature,
4. Temperature difference across insulation,
5. Outlet volumetric flow rate.

Five tubes had copper–constantan thermocouples embedded in their walls at various levels. The positioning of these tubes in the bundle is shown in Fig. 3. The center tube was equipped with four thermocouples while the remaining tubes each had two. Referring again to Fig. 3 and letting the top of the page be "north", the distance from the bottom of the bundle to each thermocouple location is given below:

Tube location	Distance from bottom of bundle, in.
Center	1·5,3,6,36
NE	3·0,36·0
SE	6·0,6·0
NW	6·0,6·0
SW	3·0,36·0

To avoid having to make tedious traverses across the tube bundle cross section to obtain the mixing-cup temperature, a mixing-cup device was constructed of light-weight cardboard sandwiched between aluminium foil. This laminated sheet was shaped into a truncated cone and a short cylinder of similar material was fitted into the smaller end of the cone (Fig. 5). A thermocouple was positioned in the lower half of this cylinder. Also, radiation shields were positioned so that the thermocouple junction could not "see" the hot tubes nor the colder objects in the room.

Outlet air flow rate was determined with a Short and Mason 4-in. dia vane anemometer which was calibrated in place above the tube bundle using rotameters as secondary standards.

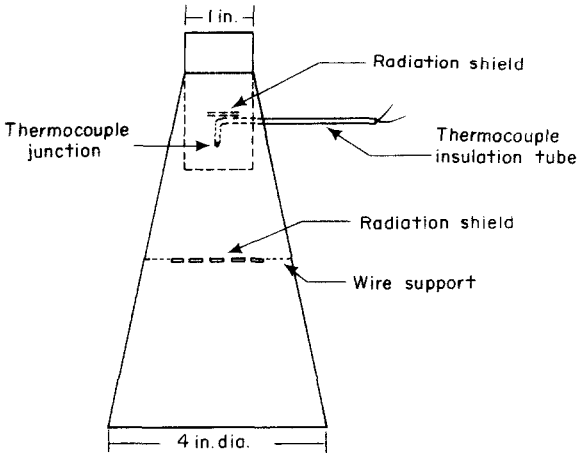

FIG. 5. Details of mixing cup.

This anemometer could measure flow rates as low as 0·5 fps with reasonable accuracy.

EXPERIMENTAL RESULTS

The data obtained from experiments on the two pitch-to-diameter ratio tube bundles were correlated in accordance with the theoretical developments for constant heat flux.

Flow rate

As noted previously, a plot of dimensionless volumetric flow rate at outlet conditions, F', vs. dimensionless length, L, produces curves parametric in pitch-to-diameter ratio but not in ξ. Figure 6 shows the results of correlating the experimental data in this manner for pitch-to-diameter ratios of 1·68 and 2·03. The heating rates represented on these two curves range from 15 to 107 Btu/hft^2. Also shown in this figure are curves obtained from the finite difference solution. Although the experimental curves have the same slope as the theoretical, they are displaced somewhat and appear to satisfy the relationship between F' and L for a smaller pitch-to-diameter ratio. This is interpreted as indicating that less area is available for flow in the experimental equipment than was assumed in the theoretical calculations. This decreased area can be attributed to the end pieces that hold the tubes in their proper triangular pitch configuration. From measurement of wall thickness of the holders and spacers, it was found that 21·0 per cent and 25·5 per cent of the requisite area was blocked out for PDR of 1·68 and 2·03, respectively. The larger percentage for PDR of 2·03 accounts for the larger disagreement between observed and theoretical values seen in Fig. 6.

Because of this decrease in flow caused by the decreased flow area in the end pieces, the boundary conditions in the theoretical calculations were altered so that $L_{(\text{theoretical})} = L_{(\text{experimental})}$. In satisfying the above, the original conditions that $P = 0$ at $Z = 0$ and $Z = L$ could no longer be satisfied without making some additional adjustments. One can think of

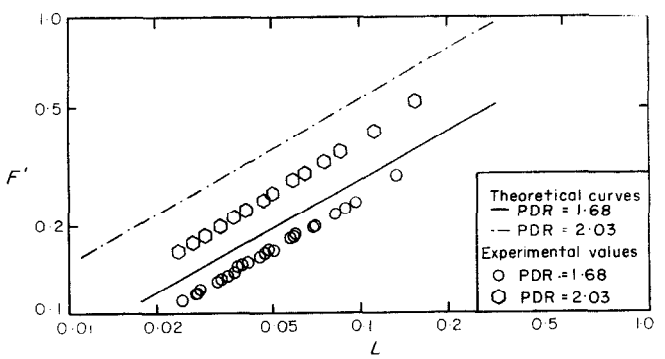

FIG. 6. Comparison of experimental and theoretical dimensionless flow rate. PDR = 1·68 and 2·03. Constant wall heat flux. $Pr = 0·7$.

the decreased flow rate being caused by an additional pressure drop attributable to the end pieces. Ideally, the pressure drop as a function of flow rate could be determined from first principles and introduced into the numerical calculations at the appropriate places and satisfy both the boundary conditions $L_{(\text{theoretical})} = L_{(\text{experimental})}$ and $P = 0$ at $Z = 0$ and $Z = L$. Since it makes no difference where the additional pressure drop is encountered, one can simply let the numerical calculations proceed until $L_{(\text{theoretical})} = L_{(\text{experimental})}$ and the additional pressure drop is determined in the process since pressure is determined at each Z increment along with the velocity and temperature profiles.

As pointed out previously, the outlet volumetric flow rate was determined using a Short and Mason vane anemometer. Having the flow rate, inlet and mean outlet temperature allowed determination of the net overall rate of heat input to the air. Combining this heating rate with physical measurements of the tube bundle and appropriate fluid properties yields Gr^*, the modified Grashof number. From the definition of F, it is seen that the above information is sufficient to determine the ordinate and abscissa for the correlations in Fig. 6.

The heat input was taken as the correct value of the heating rate to use in determining the characteristic temperature difference, Δt. The heat losses encountered were less than ten per cent of the heat input for the larger pitch-to-diameter ratio bundle. Ignoring this loss which is, in effect, a deviation from the assumed infinite array of tubes, does not introduce serious error into the correlations.

Nusselt correlation

Figures 7 and 8 compare the experimental values of local Nusselt number with those obtained from the numerical solution for PDR of 1·68 and 2·03 respectively. Since the theoretical curves of Nu as a function of a modified Graetz number are parametric in F', curves representative of the largest and smallest values of the outlet dimensionless flow rate are presented for each pitch-to-diameter ratio.

Each group of points represent temperature measurements at four axial positions in the bundle: 1·5, 3·0, 6·0 and 36·0 in. from the bottom.

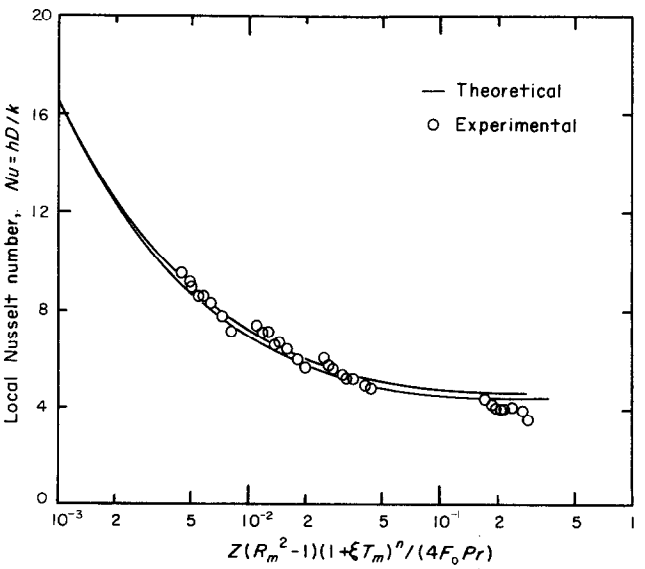

FIG. 7. Comparison of experimental and theoretical local Nusselt numbers. PDR = 2·03, $Pr = 0{\cdot}7$.

Since the heating elements were positioned approximately $\frac{3}{8}$-in. from the bottom end of each tube and because the end piece tends to keep the velocity profile flat for the first $\frac{1}{2}$ in. of the bundle, the Z position used to determine the abscissa in Figs. 7 and 8 are measured from the top of the lower end piece. The tube wall temperatures were obtained using thermocouples and 155°F, respectively. The higher experimental values can be attributed to three possible mechanisms: (1) axial conduction in the tube wall, (2) conduction error in the thermocouple leads, and (3) decreased air flow rate due to the influence of the end pieces.

The effect of (1) and (2) *should* increase with increasing heat flux while the influence of (3) on

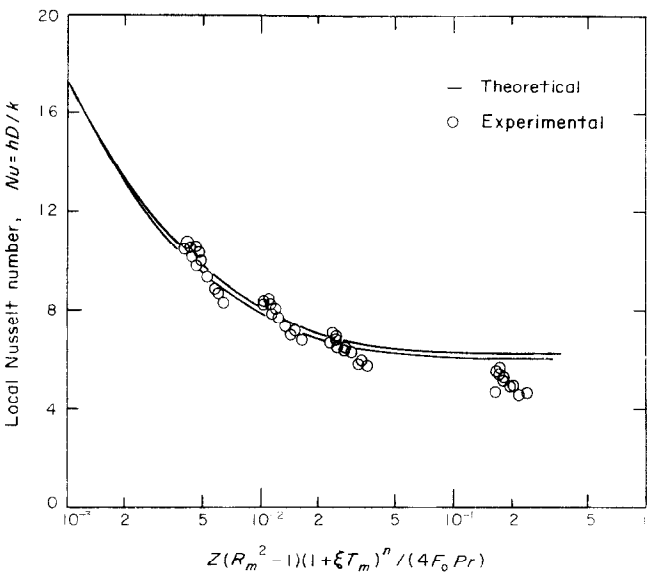

FIG. 8. Comparison of experimental and theoretical local Nusselt numbers. PDR = 1·68, Pr = 0·7.

embedded in the tube wall while the local mean air temperature was determined by assuming a linear temperature variation with axial position and by knowing inlet and mean outlet temperature.

Agreement between the experimental values and theoretical curves is quite good except for those values associated with temperature readings at the axial position three feet from the bottom of the tube bundle. Maximum disagreement is 25 per cent for the worst run: PDR = 1·68, $(q/A)_w$ = 40 Btu/hft^2. Experimental and predicted wall temperatures for this case are 160°F the Nusselt number is slight at any value of the heat flux. However, the experimental results show better agreement for this three-foot position at higher heating rates. The reason for this behaviour is not certain.

CONCLUSIONS

The effect of physical property variations on the behaviour of dimensionless flow rate as a function of modified Grashof number can be removed by correlating the outlet value of F (i.e. F') with dimensionless tube bundle length.

Local Nusselt numbers show a strong para-

metric dependence on pitch-to-diameter ratio and a weak dependence on dimensionless flow rate.

Obstructions, such as tube holders or spacers in the tube bundle, have a pronounced effect on the flow rate through the bundle but do not greatly influence the predictability of the local Nusselt numbers.

REFERENCES

1. L. P. Davis and J. J. Perona, Development of free convection flow of a gas in a heated vertical open tube, *Int. J. Heat Mass Transfer* **14**, 889–903 (1971).
2. A. J. Friedland and C. F. Bonilla, Analytical study of heat transfer rates for parallel flow of liquid metals through tube bundles, *A.I.Ch.E.Jl* **7**, 107–122 (1961).
3. L. P. Davis, Development of free convection flow through a tube bundle, Ph.D. Dissertation, The University of Tennessee (1967).
4. *Chemical Engineers' Handbook*, 3rd. ed., pp. 270 and 461. McGraw-Hill, New York (1950).
5. E. M. Sparrow and J. L. Gregg, Variable fluid-property problem in free convection, *Trans. ASME* **80**, 879–886 (1958).

DÉVELOPPEMENT D'UN ÉCOULEMENT AXIAL PAR CONVECTION NATURELLE À TRAVERS UN FAISCEAU TUBULAIRE

Résumé—Un faisceau ouvert de tubes est immergé dans un fluide. Ces tubes, orientés verticalement génèrent de la chaleur et le fluide entrant par la base du faisceau, à vitesse et température uniformes, s'écoule vers le haut extérieurement aux tubes. L'écoulement est supposé être permanent et laminaire. Les équations de couche limite thermique sont résolues pour des rapports pas/diamètre de 1,2 et 2,0 le fluide étant de l'air et la masse volumique, la viscosité et la conductivité thermique pouvant varier avec la température.

Les nombres de Nusselt locaux ont été déterminés en fonction d'un nombre de Graetz modifié et montrent la dépendance paramétrique au rapport pas diamètre et au débit adimensionnel.

Les relations entre le débit adimensionnel et la longueur du faisceau de tubes sans dimension ne sont pas modifiées par les propriétés physiques variables si le débit adimensionnel est évalué aux conditions externes.

Des expériences menées sur deux faisceaux de tubes (les rapports pas/diamètre étant de 1,68 et 2,03) sous la condition de flux thermique constant à la paroi vérifient les estimations théoriques des nombres de Nusselt. Les flux estimés se placent au-dessous des courbes calculées à cause de la réduction de la section de passage du fluide dues à l'entretoise d'écartement.

ENTWICKLUNG EINER FREIEN AXIALEN KONVEKTIONSSTRÖMUNG DURCH EIN ROHRBÜNDEL

Zusammenfassung—Ein offenes Rohrbündel wird in ein Fluid getaucht. Die Rohre, die senkrecht gerichtet sind, erzeugen Wärme und das Fluid dringt am unteren Ende des Bündels mit gleichmässiger Geschwindigkeit und Temperatur ein und fliesst ausserhalb der Rohre durch das Bündel nach oben. Es wird stabile, laminare Strömung vorausgesetzt. Die thermischen Grenzschichtgleichungen wurden für Verhältnisse Abstand/Durchmesser von 1,2 bis 2,0 mit Luft als Fluid gelöst. Luft ermöglicht es, die Dichte, Viskosität und Wärmeleitfähigkeit mit der Temperatur zu verändern.

Lokale Nusselt-Zahlen wurden auf eine modifizierte Graetz-Zahl bezogen, sie waren abhängig von den Parametern Abstand/Durchmesser und dimensionsloser Durchfluss.

Die Wechselbeziehungen zwischen dimensionslosem Durchfluss und dimensionsloser Rohrbündellänge blieben unberührt von den Betrachtungen veränderlicher physikalischer Eigenschaften, vorausgesetzt, die dimensionslosen Durchflüsse wurden bei Ausflussbedingungen ausgewertet.

Experimente, die an zwei Rohrbündeln (Abstand/Durchmesser Verhältnis von 1,68 und 3,03) bei konstantem Wärmefluss von der Wand durchgeführt wurden, bestätigten die theoretischen Aussagen der Nusselt-Zahlen. Berechnete Strömungsverhältnisse lagen unter den berechneten Kurven, da von den Rohrzwischenräumen Verengungen im Strömungsgebiet verursacht wurden.

РАЗВИТИЕ СВОБОДНО-КОНВЕКТИВНОГО ОСЕСИММЕТРИЧНОГО ТЕЧЕНИЯ СКВОЗЬ ПУЧОК ТРУБ

Аннотация—Открытый пучок труб погружен в жидкость. При выделении тепла в вертикально расположенных трубах жидкость поступает в нижнюю часть пучка с пос-

тоянной скоростью и температурой и поднимается вверх по почху вне труб. Предпогагается, что течение устойчивое и ламинарное. Уравнения теплового пограничного слоя решаются для отношений шага к диаметру от 1,2 до 2,0, когда в качестве жидкости используется воздух, причем допускается изменение плотности, вязкости и теплопроводности с изменением температуры.

Определялась зависимость локальных значений числа Нуссельта от модифсцированного числа Грэтца, и найдена параметрическая зависимость как от отношения шага к диаметру, так и от безразмерной скорости потока.

На зависимость безразмерной скорости потока от безразмерной длины пучка труб не влияют переменные физические свойства при условии, если безразмерные скорости течения вычислчлись по условиям на выходе.

Теоретические расчеты значений числа Нуссельта были проверены экспериментально на двух пучках труб с отношением шага к диаметру 1,68 и 2,03 при постоянном тепловом потоке на стенке. Полученные скорости потока располагаются ниже расчетных кривых за счет сужения сечения потока, вызванного устройством для фиксации шага.